An Analytical Approach to Objectively Sizing Cracks using Ultrasonic Phased Array Data

Journal:	*54th Annual Conference of the British Institute for Non-Destructive Testing*
Manuscript ID:	NDT-0033-2015.R1
Topic:	Theoretical Modelling
Date Submitted by the Author:	07-Aug-2015
Complete List of Authors:	Tant, Katherine; The University of Strathclyde, Mathematics and Statistics
Keywords:	Theoretical Modelling, Ultrasonic waves, Ultrasonic testing, Scattering

An analytical approach to objectively sizing cracks using ultrasonic phased array data

Katherine M. M. Tant and Anthony J. Mulholland
Department of Mathematics and Statistics,
The University of Strathclyde
Glasgow, G1 1XH, U.K.
0141 548 3647
katy.tant@strath.ac.uk

Anthony Gachagan
Centre of Ultrasonic Engineering,
The University of Strathclyde
Glasgow, G1 1XH, U.K.

Abstract

Ultrasonic phased array systems are becoming increasingly popular as tools for the non-destructive evaluation of safety-critical structures. The data captured by these arrays can be analysed to extract information on the existence, location and shape of defects. However, many of the existing imaging algorithms currently used for this purpose are heavily reliant on the choice of threshold at which the defect measurements are made and this aspect of subjectivity can lead to varying defect characterisations between different operators. To combat this, the work presented here uses the Born approximation to derive a mathematical expression for the crack size given the width of the pulse-echo response lobe of the frequency domain scattering matrix. These scattering matrices can be easily extracted from experimental data if the location of the flaw is known *a priori* and so the method has been developed exclusively for the objective characterisation of flaws. Due to the analytical nature of this work, conclusions can be drawn on the formula's sensitivity to various experimental parameters and these are corroborated using synthetic data. The sizing of a subwavelength crack is undertaken and it is shown that examination of the scattering matrix correctly captures the crack form of the defect and outperforms the standard TFM in this regard (the nature of the defect is obscured by side lobes in the TFM image). It is also suggested that the derived formulae could potentially be used to inform and optimise array design.

1. Introduction

The detection of defects within welds is vital for the life extension and reliable operation of safety critical structures such as those found in the nuclear, oil, and aerospace industries[1] [2] [3]. Ultrasonic testing is a cost-effective approach which uses

high frequency mechanical waves to inspect key components without compromising their integrity. The development of ultrasonic phased array transducers and the subsequent collection of full matrix capture (FMC) data[4] has allowed advances in the way that the interiors of these components are reconstructed. Using imaging algorithms (such as the total focussing method[4] or phase coherent imaging[5]) it is possible to detect and characterise internal defects, with techniques for improving signal to noise ratio and probability of detection continually being developed. However, one disadvantage to these imaging algorithms is the reliance on the choice of a dynamic threshold at which defect measurements are taken. Typically, large defects are measured at the -6dB threshold[6]. However, in the case of subwavelength defects, the flaw often fails to exhibit amplitudes above this threshold and there lacks a standard procedure for measuring these. Thus an aspect of ambiguity is introduced which can cause varying characterisations between operators.

An alternative to image based crack sizing has previously been examined by Zhang et al[7] and it was shown empirically that a correlation existed between the crack length and the properties of its associated scattering matrix; both the maximum scattering amplitude and the half-width, half-maximum (HWHM) measurement of the pulse-echo response (the diagonal of the scattering matrix) were shown to change monotonically with crack length. In this paper a mathematical expression for the crack size as derived from the Born approximation is discussed. The analysis of the objective model-based method developed in previous work by the authors[8], which exploits the roots of the pulse-echo response to allow the formulation of an explicit mathematical expression for crack length as opposed to a numerically derived relationship, is extended. This model based approach eliminates all aspects of subjectivity in the measurement of cracks and allows analytical conclusions on the effects of varying the system parameters to be drawn. To corroborate the conclusions drawn from the analysis, simulations of ultrasonic phased array inspections have been created in the finite element package PZFlex (Weidlinger Associates, CA) and the results are discussed in Section 3.

2. Model Based Crack-Sizing

To facilitate this analytical approach to crack-sizing, a mathematical model has been investigated. The Born approximation is a widely accepted scattering model taken originally from quantum mechanics and is based on the assumption that, within the scatterer, the scattered field is comparatively small to the incident field, which hence allows the total field to be approximated by the incident field only. Thus it is a single scattering approximation which assumes the wave passes through the flaw undisturbed (it neglects interactions between multiple flaws and between any two parts of the same flaw) and relies on the flaw medium having similar material properties to that of the host medium. However, as attention is restricted to waves in the backscattered direction (due to the limited angles of inspection typically available within an NDT setting), the discordant effects of the scattering as the wave passes through the flaw can be neglected and thus the Born approximation is valid for our purposes[9]. The model estimates the scattering amplitude arising from an incident wave (traveling in a homogeneous host medium) of given direction coming into contact with a flaw and relates the flaw response directly to the flaw geometry.

2.1. The Born Approximation

For the purposes of this work, the scattering of a pressure wave by an ellipsoidal inclusion in an elastic medium is considered. Restricting attention to the two dimensional plane below the linear array, this is given by the equation[10]

$$A(\boldsymbol{e}_i, \boldsymbol{e}_s) = -\frac{a_1 a_2 B_{lm} f_l(\boldsymbol{e}_i, \boldsymbol{e}_s)}{|\boldsymbol{g}|^2 (r_s)^2} \frac{(\sin(k_0|\boldsymbol{g}|r_s) - k_0|\boldsymbol{g}|r_s \cos(k_0|\boldsymbol{g}|r_s))}{k_0|\boldsymbol{g}|r_s} \quad \ldots\ldots\ldots\ldots(1)$$

where $\boldsymbol{e}_i, \boldsymbol{e}_s$ are unit vectors in the transmit and receive directions respectively, a_1, a_2 are the flaw dimensions, $\boldsymbol{g} = \boldsymbol{e}_i - \boldsymbol{e}_s$, the $B_{lm} f_l(\boldsymbol{e}_i, \boldsymbol{e}_s)$ term is dependent on the material properties[10], k_0 is the wave speed in the host medium and r_s is the effective radius of the flaw, given by

$$r_s = \sqrt{a_1^2 (\boldsymbol{e}_q \cdot \boldsymbol{u}_1)^2 + a_2^2 (\boldsymbol{e}_q \cdot \boldsymbol{u}_2)^2} \quad \ldots\ldots\ldots\ldots\ldots\ldots\ldots\ldots(2)$$

where $\boldsymbol{e}_q = \boldsymbol{g}/|\boldsymbol{g}|$ (note $\boldsymbol{e}_q = \boldsymbol{e}_i$ in the pulse-echo case where $\boldsymbol{e}_i = -\boldsymbol{e}_s$) and $\boldsymbol{u}_1, \boldsymbol{u}_2$ are unit vectors along the major and minor axis of the flaw respectively.

2.2.1 Scattering Matrices

The Born approximation provides an explicit expression for the scattering amplitude A of a scattered pressure wave between a pair of transmit/receive array elements at a specified frequency. Plotting the magnitude of this amplitude for every pair of array elements produces a scattering matrix. This matrix contains information on the characteristics of the defect[11] and the patterns observed can be exploited to extract information on its size, shape and orientation.

2.2. A mathematical expression for crack-size

From the Born approximation given in equation (1) the following expression for the crack length $a = 2a_1$ can be derived

$$a = \sqrt{\frac{M^2\lambda^2}{4\pi^2} \csc^2(\phi_i + \theta) - 4a_2^2 \cot^2(\phi_i + \theta)} \quad \ldots\ldots\ldots\ldots\ldots\ldots\ldots..(3)$$

where M=4.49341[8], λ is the wavelength, θ is the crack orientation (relative to the x axis) and $\phi_i = \operatorname{atan}(x_i/r)$, the angle between the vertical axis and the vector connecting the centre of the flaw at depth r to the element at which the root occurs along the pulse-echo response (denoted x_i- see Figure 1). Note, there exist two unknowns, the crack length a and the orientation θ. However, as there exist two roots of the pulse-echo response, the equation

$$\frac{M^2\lambda^2}{16\pi^2} \csc^2(\phi_1 + \theta) - a_2^2 \cot^2(\phi_1 + \theta) = \frac{M^2\lambda^2}{16\pi^2} \csc^2(\phi_2 + \theta) - a_2^2 \cot^2(\phi_2 + \theta) \quad (4)$$

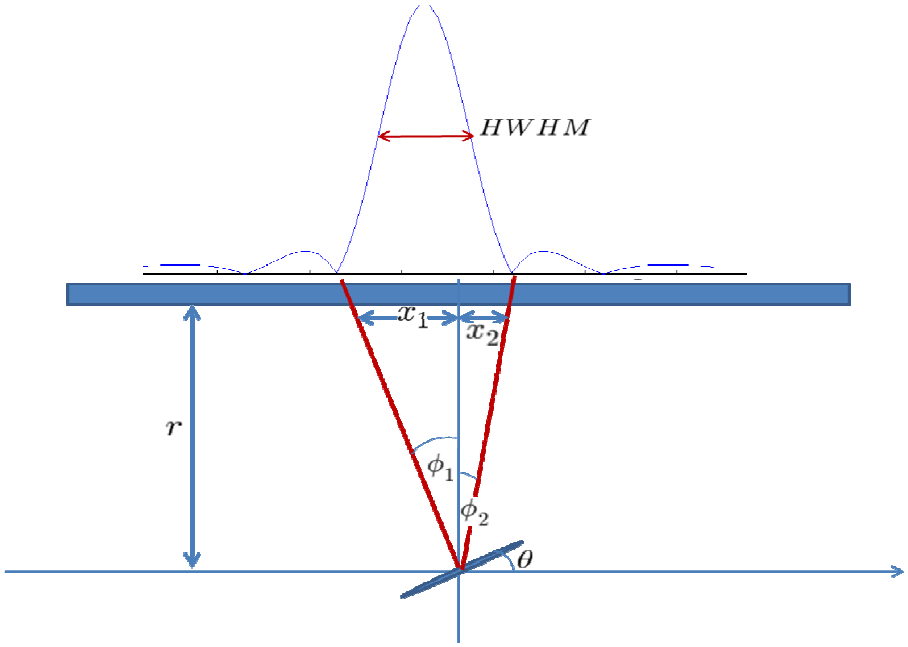

Figure 1. Schematic demonstrating the relationship between the elements at which the roots of the pulse-echo response occur (x_1 and x_2), the depth r and the angles ϕ_1 and ϕ_2.

can be solved for ϑ and this value can subsequently be substituted into equation (3) to elicit the crack length a. Due to the restriction of interest to crack-like flaws, where $a_1 \gg a_2$, the condition

$$\frac{a}{\lambda} > \frac{M}{2\pi} > \frac{2a_2}{\lambda} \quad \text{.....(5)}$$

must be adhered to[8]. This lower bound on the crack length to wavelength ratio gives the minimum resolvable crack length for the method, a measure which could potentially be used for comparison with other methods in terms of resolution. Furthermore, an explicit expression predicting the angle at which the root of the pulse-echo lies can also be derived

$$\phi_i = \pm \sin^{-1}\left(\sqrt{\frac{M^2\lambda^2 - 16\pi^2 a_2^2}{16\pi^2(a_1^2 - a_2^2)}}\right) - \theta, \quad \text{.....(6)}$$

where the positive branch gives ϕ_2 and the negative branch gives ϕ_1 (see Figure 1). Relating these to element locations ($x_i = r\tan\phi_i,\ i = 1,2$), the minimum array length required to capture both these roots (necessary for the extraction of an accurate estimation of orientation and length) can be written

$$L_{min} = r|\tan\phi_1 - \tan\phi_2|. \quad \text{.....(7)}$$

Additionally, the error of the method caused by the extent of the discretisation of the array (i.e. the array pitch p) can be approximated by the expression[8]

$$\varepsilon^A = \left| \frac{M^2(p^2 - 2x_i p) - 16\pi^2 \left(\frac{a_2}{\lambda}\right)^2 p \sin\theta (p\sin\theta - 2x_i \sin\theta + 2r\cos\theta)}{8\pi^2 \frac{a}{\lambda}(x_i \cos\theta + r\sin\theta)^2} + \frac{\frac{a}{\lambda} p\cos\theta}{x_i \cos\theta + r\sin\theta} \right|. \quad \ldots(8)$$

The work in this paper revolves around the sizing of subwavelength defects using scattering matrices and the assessment of equations (5)-(8), exploring whether they can be reliably used to guide experimental procedure.

3. Results

To corroborate the analytical conclusions drawn above, the finite element software package PZFlex was used to generate two separate FMC datasets from a two dimensional simulation of a phased array inspection of a steel block. The parameters used in each simulation can be found in Table 1.

Table 1. Parameters used in the software package PZFlex to simulate the phased array inspection of a steel block.

Parameter	Dataset A	Dataset B
Number of Array Elements	64	64
Array Pitch	1mm	1mm
Transducer centre frequency	3Mhz	3MHz
Wave speed in host material	5900ms^{-1}	5900ms^{-1}
Density of host material	7900kg/m^3	7900kg/m^3
Depth of sample	60mm	60mm
Time step	9ns	9ns
Flaw length	5mm	1.4mm
Flaw depth	20mm	30mm

Frequency domain scattering matrices are easily extracted from these FMC datasets. Assuming the location of the flaw is known *a priori,* the distance to the centre of the flaw can be calculated for each transmit-receive pair; this dictates the centre of the time window on which the FFT is performed. In the work below, where the host material is perfectly homogeneous and the flaw is located at a good distance from the back wall, a large time window can be taken without including scattering by artefacts other than the flaw (here a square box of 7mm length is centred around the flaw and data pertaining to this spatial zone is used). However, in cases where there exist multiple scatterers, it is recommended a smaller time window is used. Once the data has been transformed into the frequency domain, the amplitude at a specified frequency for each transmit-receive

pair is plotted to generate a scattering matrix. For the formula derived in this paper, only the pulse-echo response (the diagonal of the scattering matrix) is required (that is, when $\boldsymbol{e_i = -e_s}$).

3.1 Application of the Crack Sizing Formula

To begin, the crack sizing algorithm is applied to both datasets described in Table 1. Note that $\boldsymbol{a_2}$ is set equal to zero in equation (3) as the inspection concerns a zero volume flaw (the term is retained only to allow further generalisation of the method to elliptical flaws with high aspect ratios, for example long slots). For dataset A the scattering matrix is examined at the centre frequency of the transducer, 3MHz. Figure 2 (a) shows the resulting pulse-echo response (blue line). Due to noisy experimental effects (scattering by the back wall, transduction effects, mode conversion etc.), it can be difficult to approximate the innermost root of the pulse-echo response as several local minima exist. For the purposes of the work shown in this paper, the gradient at the HWHM is measured and then projected onto the x-axis (as demonstrated by the dashed lines in Figure 2 (a)). The intercept is then taken to be the estimated root. For dataset A, the root occurs at element 39 which equates to 6.5mm along the $\boldsymbol{x}$-axis (the array is centred at the origin). Using this value to calculate $\boldsymbol{\phi_2}$ (from Figure 1 it is obvious that $\boldsymbol{\phi_2 = \tan^{-1}(x_2/r)}$), and subsequently $\boldsymbol{a}$, a crack length estimate of 4.6mm is achieved, exhibiting an 8% error from the actual crack length of 5mm.

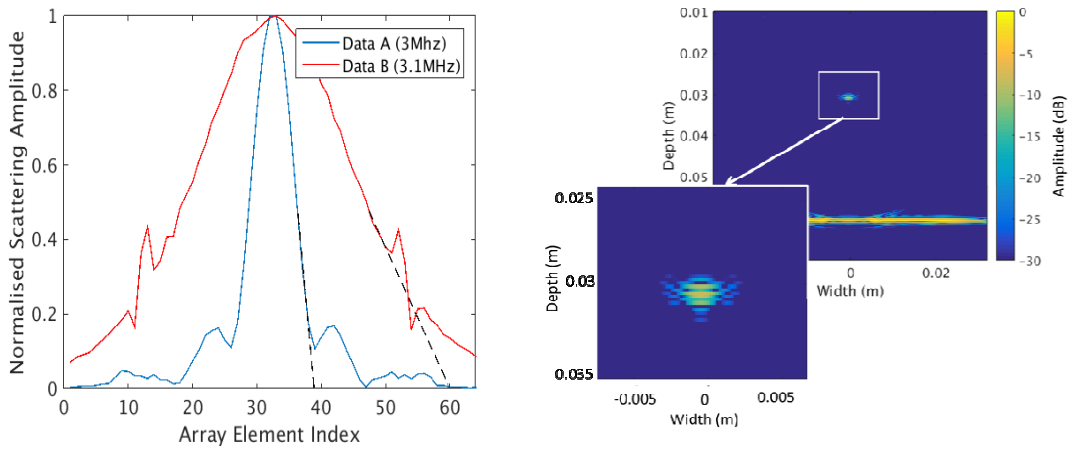

(a) (b)

Figure 2. (a) Pulse-echo responses from the scattering matrices arising from dataset A at 3MHz (blue line) and dataset B at 3.1MHz (red line). The dashed lines demonstrate how the root is estimated. (b) TFM image of the 1.4mm crack in dataset B.

For dataset B, to test the limits of the method's resolution, the scattering matrix is examined at 3.1MHz so as to give a crack length to wavelength ratio of $\boldsymbol{a/\lambda = 0.737}$, close to the lower bound on the minimum resolvable crack length condition as given in equation (5). The root is estimated to occur at element 60 (see Figure 2 (a), red line), equating to $\boldsymbol{x_2 = 27.5}$ mm along the $\boldsymbol{x}$-axis. Calculating $\boldsymbol{\phi_2}$ from this value and substituting it into equation (3) (letting $\boldsymbol{a_2 = 0}$) the crack length estimate obtained is

a =2mm (recall the known crack size is 1.4mm). To measure the relative success of the algorithm in this case, the standard TFM was also applied to dataset B. Figure 2 (b) displays the resulting images, plotted with a dynamic range of 30dB, and it can be seen that prominent side lobes obscure the form of the defect; it is not possible to determine that it is a crack. Returning to Figure 2 (a), the form of the pulse-echo response curve here tells us unequivocally that the defect is crack-like (if the flaw was a disc the scattering matrix would exhibit a stripe rather than an elliptical high amplitude lobe and this information is retained in the pulse-echo responses – see Figure 3). It is thus shown that the use of scattering matrices to help characterise defects can enhance the information extracted from the TFM reconstruction of the flaw.

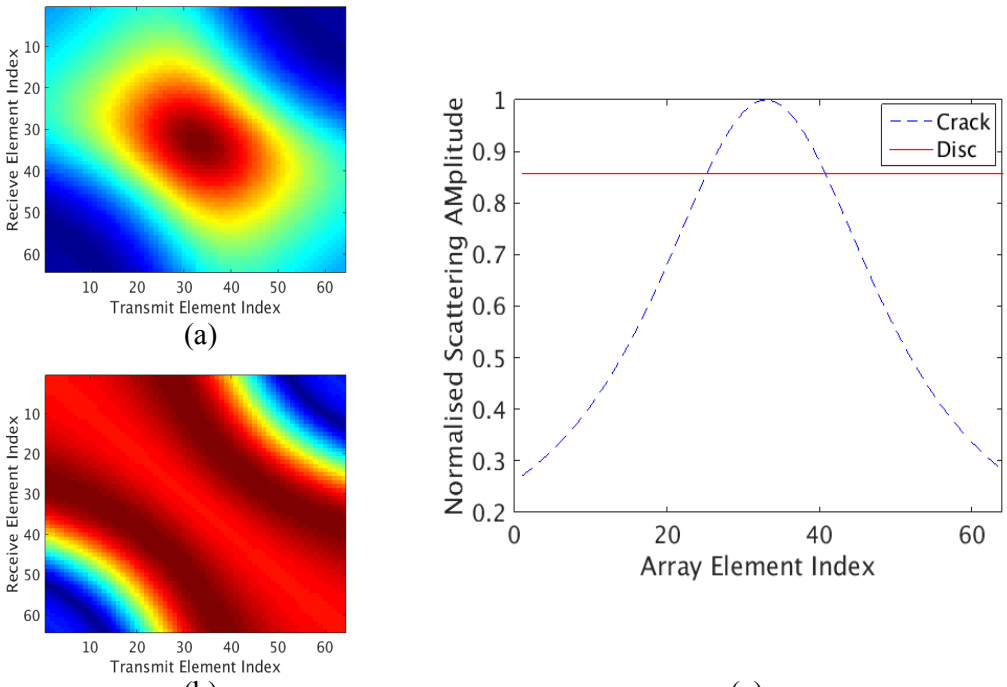

Figure 3. Model scattering matrices (as calculated by the Born approximation) arising from (a) a 1.4mm crack and (b) a disc with diameter 1.4mm, both plotted at 3.1MHz. Plot (c) displays the corresponding pulse-echo responses.

3.2 Crack-sizing Error Caused by Array Pitch

From equation (3) it is clear that a reliable estimation of ϕ_i is necessary to obtain an accurate crack length estimate. Due to limitations on transducer design, it is not possible to observe the scattering amplitude over a continuous range of angles; the angles of observation are dictated by the array pitch. Thus, the root of our pulse-echo response (on which ϕ_i is dependent) is approximate, the accuracy of the approximation being dependent on the extent of the array pitch.

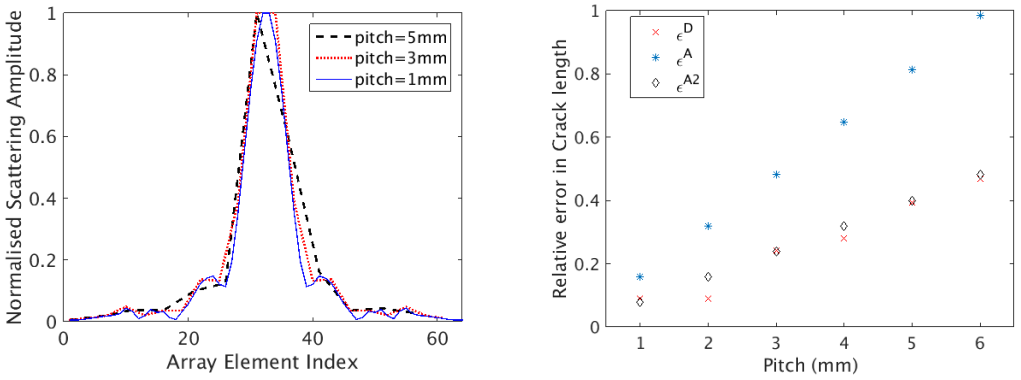

(a) (b)

Figure 4. (a) Plots of the pulse-echo response taken from subsets of the FMC data arising from dataset A, demonstrating the distortion caused by an increase in array pitch. (b) Plot of the analytically derived error assuming the approximated root is out by a pitch (ϵ^A) and half a pitch (ϵ^{A2}). The actual error obtained via extraction of the roots from the pulse-echo is also plotted (ϵ^D).

Equation (8) provides an analytical expression for the upper bound on the error caused by this discretisation. To assess it, a simulation was run in PZFlex using the parameters as listed in Table 1 for dataset A. By taking subsets of the FMC it is possible to artificially alter the array pitch. For example, using the transmit/receive data from every second element doubles the gap between neighbouring elements, mimicking an array with a 2mm array pitch. Creating scattering matrices from these reduced FMCs, the pulse-echo responses can be plotted and it can be observed in Figure 4 (a) that the greater the gap between array elements, the more distorted the pulse-echo response becomes. Extracting the roots, the crack-sizing formula can be applied and the resulting relative errors calculated. These are plotted in Figure 4 (b) in red (ϵ^D) whilst the analytically derived upper bound on the error is plotted in blue (ϵ^A). It can be observed that the analytically derived error is a strict upper bound in all cases. However, this is the worst case scenario and in practice it is more likely that the approximate root is out by only half of the array pitch rather than the full array pitch[8]. Replacing p by $p/2$ in equation (8) results in ϵ^{A2}, which although not a strict upper bound, does provide a better prediction for the actual error obtained.

3.3 Minimum Array Length Required

From Figure 2 (a) it can be seen that the lower the crack length to wavelength ratio, a/λ, the wider the lobe of the pulse-echo response. To accurately size a flaw, it is imperative that the array captures the location of the innermost roots. Hence, given a lower bound on the crack sizes of interest, the minimum array aperture required can be estimated using equation (7). For example, for dataset B the minimum array length required to correctly capture the roots of the pulse-echo response is calculated as 55.7mm. In dataset A, the minimum array length required is estimated as 12.8 mm. These are both in agreement with Figure 2 (a), roughly corresponding with the width of the high amplitude lobes. This estimation could be useful in array transducer design;

given a centre frequency and a lower bound on the crack lengths that are deemed of interest, the minimum array length required to capture all facets of the defect can be obtained. Additionally, when used in conjunction with equation (8) to dictate an acceptable margin of error, this can be combined with an optimum array pitch. This could potentially inform the design for sparse arrays.

4. Conclusions

This paper further examines the analytical crack-sizing method previously developed by the authors[8], focussing primarily on its application to small flaws and the validation of the upper error bound caused by the extent of the array pitch. Synthetic data was created by simulating a phased array inspection of a steel block in the finite element package PZFlex. Initially, a 5mm horizontal crack was embedded 20mm from the array. The crack-sizing formula estimated its length at 4.6mm, giving rise to an error of 8%. Subsets of this FMC data were then taken, artificially altering the array pitch. It was thus shown that the expression for the error dependent on the array pitch was a strict upper bound. Additionally, substituting a half pitch into this equation gave rise to a more accurate estimation for the actual error obtained. A second simulation was then executed, this time including a crack of length 1.4mm, located 30mm below the array. This gave rise to a crack length to wavelength ratio of $a/\lambda = 0.737$, close to the limit of the method's minimum resolvable crack length. Although traditional imaging algorithms can often detect these small flaws, it is often not possible to apply the standard measuring protocols used for large flaws. Additionally, the nature of subwavelength flaws can often be obscured using traditional imaging algorithms due to the presence of side lobes. On inspection of the pulse-echo response of the scattering matrix arising from the subwavelength flaw, it was possible to determine unequivocally that the defect was in fact a crack – a detail not obvious from the TFM image. The crack-sizing formulae subsequently gave rise to a crack length estimate of 2mm. Although the relative error here is not negligible, the method proved relatively successfully in comparison with the standard TFM. It must also be noted that the current model does not account for effects such as mode conversion, transduction effects or multiple scattering, and introducing such effects to build a more sophisticated analytical model could further improve the method's performance. Finally, some comment was made on the potential use of the derived formulae to guide transducer design. Given constraints on the defect size of interest and the desired centre frequency of a transducer, the formulae derived in this paper could be used to determine the optimal array length and pitch. This could be particularly useful in the design of sparse arrays.

Acknowledgements

This work was funded through the UK Research Centre in NDE Targeted Programme by the Engineering and Physical Sciences Research Council (grant number EP/IO19731/1), Amec Foster Wheeler, National Nuclear Laboratory, Rolls Royce, Shell, and Weidlinger.

References

1. M Cherfaoui, 'Innovative techniques in non-destructive testing and industrial applications on pressure equipment′, Procedia. Eng, Vol. 46, pp. 266-278, 2012.
2. J Davies and P Cawley 'The application of synthetic focusing for imaging crack-like defects in pipelines using guided waves,' IEEE TUFFC, Vols. 56, No 4, pp. 759-771, 2009.
3. U Schnars and R Henrich, 'Applications of NDT methods on composite structures in aerospace industry', Conf. on Damage in Composite Materials, Stuttgart, Germany, pp. 1-8, 2006.
4. C Holmes B W Drinkwater P D Wilcox, 'Post-processing of the full matrx of ultrasonic transmit receive array data for nondestructive evaluation', NDT Int, Vol 38, No 8, pp. 701-711, 2005.
5. J Camacho, M Parrilla and C Fritsch, 'Phase Coherent Imaging', IEEE TUFFC, Vol 56, No 5, pp 958-974, 2009.
6. P D Wilcox, C Holmes and B W Drinkwater, 'Advanced reflector characterisation with ultrasonic phased arrays in NDE applications', IEEE TUFFC, Vol 54, No 8, pp 1541-1550, 2007.
7. J Zhang, B W Drinkwater and P D Wilcox, 'The use of ultrasonic arrays to characterise crack-like defects', J. NDE, Vol 29, No 4, pp. 222-232, 2010.
8. K M M Tant, A J Mulholland, A Gachagan, 'A Model-Based Approach to Crack Sizing With Ultrasonic Arrays', IEEE TUFFC, Vol 62, No 5, pp. 915-926, May 2015
9. J E Gubernatis, E Domany, J A Krumhansl and M Huberman, 'The Born Approximation in the Theory of the Scattering of Elastic Waves by Flaws', J. App. Phys., Vol 48, No 7, pp. 2812-2819, 1977.
10. L W Schmerr, 'Fundamentals of Ultrasonic Nondestructive Evaluation', Plenum Press, New York, 1998.
11. J. Zhang, B W Drinkwater and P D Wilcox, 'Defect Characterisation Using an Ultrasonic Array to Measure the Scattering Coefficient Matrix', IEEE TUFFC, Vol 55, No 10, pp. 2254-2265, 2008.